


Cadmium(II) complexes of 5-nitro-salicylaldehyde and α -diimines: Synthesis, structure and interaction with calf-thymus DNA

Ariadni Zianna, Maja Sumar Ristic, George Psomas, Antonis Hatzidimitriou, Evdoxia Coutouli-Argyropoulou & Maria Lalia-Kantouri

To cite this article: Ariadni Zianna, Maja Sumar Ristic, George Psomas, Antonis Hatzidimitriou, Evdoxia Coutouli-Argyropoulou & Maria Lalia-Kantouri (2015): Cadmium(II) complexes of 5-nitro-salicylaldehyde and α -diimines: Synthesis, structure and interaction with calf-thymus DNA, Journal of Coordination Chemistry, DOI: [10.1080/00958972.2015.1101075](https://doi.org/10.1080/00958972.2015.1101075)

To link to this article: <http://dx.doi.org/10.1080/00958972.2015.1101075>

 View supplementary material 

 Accepted author version posted online: 01 Oct 2015.

 Submit your article to this journal 

 Article views: 4

 View related articles 

 View Crossmark data 

Publisher: Taylor & Francis

Journal: *Journal of Coordination Chemistry*

DOI: <http://dx.doi.org/10.1080/00958972.2015.1101075>

Cadmium(II) complexes of 5-nitro-salicylaldehyde and α -diimines: Synthesis, structure and interaction with calf-thymus DNA

ARIADNI ZIANNA[†], MAJA SUMAR RISTOVIC^{†‡}, GEORGE PSOMAS[†], ANTONIS HATZIDIMITRIOU[†],
EVDOKIA COUTOULI-ARGYROPOULOU[§] and MARIA LALIA-KANTOURI^{*†}

[†]Department of General and Inorganic Chemistry, Faculty of Chemistry, Aristotle University of Thessaloniki, GR-54124 Thessaloniki, Greece

[‡]Faculty of Chemistry, University of Belgrade, Studenski trg 12-16, Belgrade, Serbia

[§]Department of Organic Chemistry and Biochemistry, Faculty of Chemistry, Aristotle University of Thessaloniki, GR-54124 Thessaloniki, Greece

Five Cd(II) complexes with the anion of 5-NO₂-salicylaldehydeH (5-NO₂-salOH) in the absence or presence of the α -diimine 1,10-phenanthroline (phen), 2,2'-dipyridylamine (dpamH), 2,2'-dipyridine (bipy) or 2,9-dimethyl-1,10-phenanthroline (neoc) were synthesized and characterized as [Cd(5-NO₂-salO)₂(CH₃OH)₂] (**1**), [Cd(5-NO₂-salO)₂(phen)]·2CH₃OH·H₂O (**2**), [Cd(5-NO₂-salO)₂(dpamH)] (**3**), [Cd₃(5-NO₂-salO)₆(bipy)₂] (**4**) and [Cd(5-NO₂-salO)(neoc)(NO₃)₂] (**5**). Based on spectroscopic results (IR, UV, NMR), elemental analysis and conductivity measurements an octahedral geometry around cadmium metal ion is suggested, with the 5-NO₂-salicylaldehyde ligand having different coordination modes. The structures determined by X-ray crystallography verified neutral mononuclear **1-3** and trinuclear **4**. Simultaneous TG/DTG-DTA technique was used to analyze the thermal behavior of **1**, **2** and **3**. The complexes bind tightly to calf-thymus DNA mainly by intercalation, as concluded by DNA-viscosity measurements and exhibit significant displacement of EB from the EB-DNA complex.

Keywords: Cadmium(II) complexes; Crystal structure; Interaction with DNA

1. Introduction

Cadmium is considered a human carcinogen by the International Agency for Research on Cancer. Cadmium can induce cancer by a number of mechanisms, the most important among

*Corresponding author. Email: lalia@chem.auth.gr

them are aberrant gene expression, inhibition of DNA damage repair, induction of oxidative stress, and inhibition of apoptosis [1]. Cadmium accumulates in the human body with a long half-life and its targets of toxicity include bone, cardiovascular system, immune system, liver, lung and kidney [2]. These drawbacks limit research on this metal, but complexes with antimicrobial [3, 4], as well as antibacterial/antifungal properties have been reported [5]. In addition, there have been studies regarding the cytotoxic activity of a dinuclear Cd(II) complex [6], as well as Cd(II) complexes with antiproliferative [7, 8] and cancer cell inhibitory properties [9].

The interaction of transition metal complexes with DNA has been in the center of scientific interest for many years, mainly due to their potential applications in cancer research and molecular biology [10, 11] and among other metal complexes with more bio-compatible metals; the ability of cadmium complexes to bind to DNA has also been investigated [12-18].

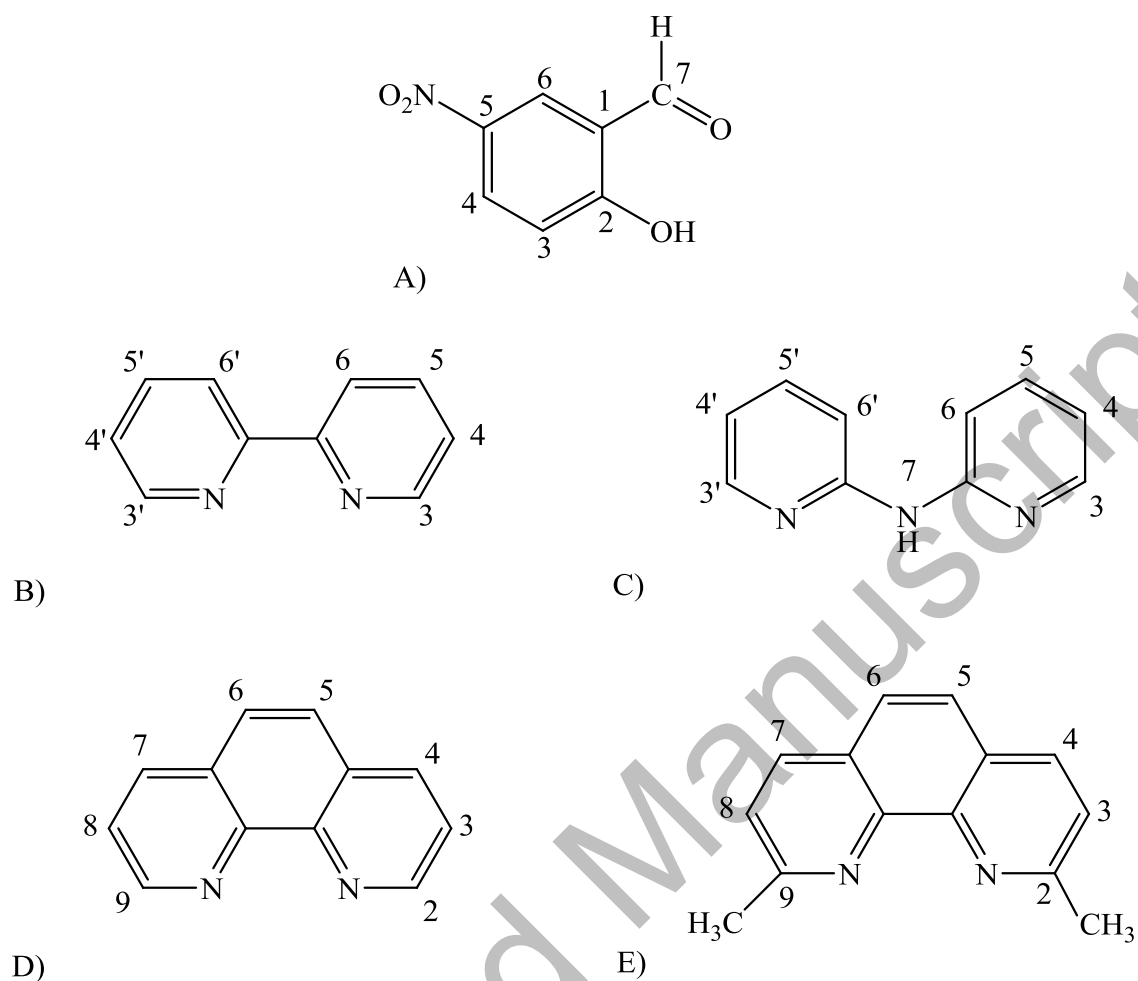
The strong coordinating properties of 2-hydroxy-benzaldehyde (salicylaldehyde) and its complexes with 3d transition metals have stimulated research on these compounds that find applications in both pure [19, 20] and applied chemistry [21, 22]. It has also been shown that these ligands possess antimicrobial properties [23, 24]. These ligands coordinate mainly in a bidentate manner with transition metals in the mono-anionic form, adopting geometries from square-planar [25] to square-pyramidal [26] and octahedral [27].

We have initiated in our laboratory the synthesis and characterization of transition metal complexes with carbonyl compounds derived from salicylaldehyde and benzophenone ligands [28-34]. Our interest is based on the synthesis of metal complexes with substituted salicylaldehydes and their interaction with DNA. Previous studies showed that zinc(II) and copper(II) complexes with substituted salicylaldehydes or 2-hydroxybenzophenones have interesting binding to calf-thymus (CT) DNA [32, 33, 35], while Co(II) complexes in the presence of the nitrogen-donor ligand 2,2'-dipyridylamine (dpamH) exhibited anticancer activity [31].

As continuation of our research, we synthesized and characterized cadmium(II) complexes with the ligand HL = 5-nitro-2-hydroxy-benzaldehyde (5-nitro-salicylaldehyde, abbreviated as 5-NO₂-salOH) in the absence [Cd(5-NO₂-salO)₂(CH₃OH)₂] (**1**), or presence of α -diimines 2,2'-dipyridine (bipy), dpamH, 1,10-phenanthroline (phen) and 2,9-dimethyl-1,10-phenanthroline or neocuproine (neoc) (scheme 1). These compounds gave different structures

according to the α -diimine used. Their characterization was achieved by physicochemical measurements and spectroscopic methods (IR, UV-vis, ^1H - and ^{13}C -NMR) and formulated as $[\text{Cd}(5\text{-NO}_2\text{-salo})_2(\text{phen})]\cdot 2\text{CH}_3\text{OH}\cdot\text{H}_2\text{O}$ (**2**), $[\text{Cd}(5\text{-NO}_2\text{-salo})_2(\text{dpamH})]$ (**3**), $[\text{Cd}_3(5\text{-NO}_2\text{-salo})_6(\text{bipy})_2]$ (**4**) and $[\text{Cd}(5\text{-NO}_2\text{-salo})(\text{neoc})(\text{NO}_3)]_2$ (**5**). The crystal structures of **1-4** were verified by single-crystal X-ray diffraction analysis. The thermal stabilities for **1-3** were investigated by simultaneous (TG/DTG-DTA) technique. The ability of the complexes to bind to calf-thymus DNA (CT DNA) has been investigated by: (i) UV spectroscopic titration studies and the binding constants to CT DNA, K_b , have been determined, (ii) measurements of the viscosity of DNA solution in the presence of increasing amounts of **1-5** and (iii) competitive binding titration with the classic intercalator ethidium bromide (EB) performed by fluorescence spectroscopy in order to assess the ability of the compounds to displace EB from the EB-DNA complex as indirect proof of a potential intercalative binding mode.

Accepted Manuscript



Scheme 1. The formula of (A) 5-NO₂-salicylic acid, (B) bipyridine, (C) dpamH, (D) phenanthroline and (E) neocuproine with the H atom numbering.

2. Experimental

2.1. Materials - Instrumentation – Physical measurements

The α -diimines (bipyridine, dpamH, phenanthroline and neocuproine), 5-NO₂-salicylic acid, Cd(NO₃)₂·4H₂O, CH₃ONa, trisodium citrate, NaCl, CT DNA and EB were obtained as reagent grade from Sigma-Aldrich Co. and were used as received. Solvents for the preparation and physical measurements of “extra pure” grade were obtained from Chemlab without further purification.

The DNA stock solution was prepared by dilution of CT DNA to buffer (containing 150 mM NaCl and 15 mM trisodium citrate at pH 7.0) followed by exhaustive stirring for three days, and kept at 4 °C for no longer than a week. The stock solution of CT DNA gave a value of A₂₆₀/A₂₈₀ (ratio of UV absorbance at 260 and 280 nm) equal to 1.85, indicating that the DNA

was sufficiently free of protein contamination [36]. The DNA concentration was determined by the UV absorbance at 260 nm after 1:20 dilution using $\epsilon = 6600 \text{ M}^{-1}\text{cm}^{-1}$ [37].

The infrared (IR) spectra ($400\text{--}4000 \text{ cm}^{-1}$) were recorded on a Nicolet FT-IR 6700 spectrometer with samples prepared as KBr pellets. The UV-visible (UV-vis) spectra were recorded as nujol mulls and in DMSO solutions at concentrations from $10^{-5}\text{--}10^{-3} \text{ M}$ on a Hitachi U-2001 dual beam spectrophotometer. ^1H -NMR and ^{13}C -NMR spectra were recorded at 300 MHz and 75 MHz, respectively, on a Bruker AVANCE^{III} 300 spectrometer using DMSO- d_6 as solvent. C, H and N elemental analyses were performed on a Perkin Elmer 240B elemental microanalyzer. Molecular conductivity measurements of 1 mM DMSO solution of the complexes were carried out with a Crison Basic 30 conductometer. Fluorescence spectra were recorded in solution on a Hitachi F-7000 fluorescence spectrophotometer. Viscosity experiments were carried out using an ALPHA L Fungilab rotational viscometer equipped with an 18 mL LCP spindle and the measurements were performed at 100 rpm. The simultaneous TG/DTG-DTA curves were recorded on a SETARAM thermal analyzer, model SETARAM SETSYS-1200. The samples of approximately 10 mg were heated in platinum crucibles, in a nitrogen atmosphere at a flow rate of 50 mL min^{-1} , from $30\text{--}900 \text{ }^\circ\text{C}$ at a heating rate of $10 \text{ }^\circ\text{C min}^{-1}$.

2.2. Synthesis of the complexes

2.2.1. Synthesis of $[\text{Cd}(5\text{-NO}_2\text{-salOH})_2(\text{CH}_3\text{OH})_2]$ (1). Complex **1** was prepared according to the published procedure [38], by addition of a methanolic solution (20 mL) of 5- NO_2 -salOH (1 mmol, 167 mg), deprotonated with CH_3ONa (1 mmol, 54 mg), to a methanolic solution (20 mL) of $\text{Cd}(\text{NO}_3)_2 \cdot 4\text{H}_2\text{O}$ (0.5 mmol, 154 mg) at room temperature. The reaction mixture was heated at $50 \text{ }^\circ\text{C}$, stirred for 1 h turning yellow. The reaction solution was left to stand at room temperature for slow evaporation and after a few days, yellow crystals suitable for X-ray structure determination were collected with filtration and air-dried. Yield 53.0%, 270 mg, analyzed as $[\text{Cd}(5\text{-NO}_2\text{-salO})_2(\text{CH}_3\text{OH})_2]$, ($\text{C}_{16}\text{H}_{16}\text{Cd}_1\text{N}_2\text{O}_{10}$) (MW=508.71): C, 37.78; H, 3.71; N, 5.51. Found: C, 37.80; H, 3.70; N, 5.52. IR spectrum (KBr): selected peaks in cm^{-1} : 3437 (medium, (m)) $\nu(\text{O-H})$ of coordinated methanol, 1641 (strong, (s)) $\nu(\text{C=O})$, 1325 (strong-to-medium (sm)) $\nu(\text{C-O}\rightarrow\text{Cd})$, 494 (m) $\nu(\text{Cd-O})$; UV-vis: λ/nm ($\epsilon/\text{M}^{-1}\text{cm}^{-1}$) as nujol mull: 370, 428; in DMSO: 373 (3270), 432 (5800); molar conductivity in 1 mM DMSO = $15.0 \mu\text{S/cm}$. ^1H -NMR (300 MHz) spectrum in DMSO- d_6 (δ/ppm): 9.88 (2H, s, H^7 5- NO_2 -salO), 8.29 (2H, d,

$J = 3.2$ Hz, H^6 5-NO₂-salo), 7.91 (2H, dd, $J = 9.6, 3.2$ Hz, H^4 5-NO₂-salo), 6.48 (2H, d, $J = 9.6$ Hz, H^3 5-NO₂-salo). ¹³C-NMR (75 MHz) spectrum in DMSO-d₆ (δ/ppm): 192.5, 179.2, 131.5, 129.3, 129.1, 125.0, 122.3.

2.2.2. Synthesis of the cadmium mixed-ligand complexes (2-5). The reaction of a methanolic solution of Cd(NO₃)₂·4H₂O with quantities of 5-NO₂-saloH in methanol (deprotonated by sodium methoxide) and an α-diimine (bipy, phen, neoc, dpamH) led to the preparation of mixed-ligand cadmium complexes (2-5).

[Cd(5-NO₂-salo)₂(phen)]·2CH₃OH·H₂O (2). Complex **2** was prepared by addition of a methanolic solution (15 mL) of 5-NO₂-saloH (1 mmol, 157 mg) deprotonated with CH₃ONa (1 mmol, 54 mg) to a methanolic solution (10 mL) of Cd(NO₃)₂·4H₂O (0.5 mmol, 154 mg) and phen (0.5 mmol, 90 mg). The reaction mixture was stirred for two hours at 50 °C and left for slow evaporation. Yellow crystals suitable for X-ray structure determination, yield 51.0%, 361 mg, analyzed as [Cd(5-NO₂-salo)₂(phen)]·2MeOH·H₂O (C₂₈H₂₆Cd₁N₄O₁₁) (MW=706.93): C, 47.57; H, 3.71; N, 7.92. Found: C, 47.59; H, 3.72; N, 7.90. IR spectrum (KBr): selected peaks in cm⁻¹: 3432 (m) ν(O-H) of crystalized methanol and H₂O, 1647(s) and 1603(s) ν(C=O), 1541(sm) ν(C=N), 1323(sm) ν(C-O→Cd), 836(m), 756(m) and 723(sm) δ(C-H)_{phen}, 529(m) ν(Cd-O); 478(m) ν(Cd-N); UV-vis: λ/nm as nujol mull: 375, 427; in DMSO: 373 (3630), 432 (4710); molar conductivity in 1 mM DMSO = 25.0 μS/cm. ¹H-NMR (300 Hz) spectrum in DMSO-d₆ (δ/ppm): 10.08 (2H, s, H^7 5-NO₂-salo), 8.28 (2H, d, $J = 3.2$ Hz, H^6 5-NO₂-salo), 7.95 (2H, dd, $J = 9.5, 3.2$ Hz, H^4 5-NO₂-salo), 6.57 (2H, d, $J = 9.5$ Hz, H^3 5-NO₂-salo) and 9.07 (2H, d, $J = 4.3$ Hz, H^2 and H^9 phen), 8.87 (2H, d, $J = 8.2$ Hz, H^4 and H^7 phen), 8.25 (2H, s, H^5 and H^6 phen), 8.04 (2H, dd, $J = 8.2, 4.3$ Hz, H^3 and H^8 phen). ¹³C-NMR (75 MHz) spectrum in DMSO-d₆ (δ/ppm): 191.0, 176.2, 150.0, 148.9, 139.8, 133.1, 129.5, 128.9, 128.2, 127.2, 125.4, 123.2, 122.4.

[Cd(5-NO₂-salo)₂(dpamH)] (3). Yellow crystals suitable for X-ray structure determination, yield 57.0%, 351 mg, analyzed as [Cd(5-NO₂-salo)₂(dpamH)], (C₂₄H₁₇CdN₅O₈) (MW=615.83): C, 46.81; H, 2.78; N, 11.37. Found: C, 46.85; H, 2.79; N, 11.36. IR spectrum (KBr): selected peaks in cm⁻¹: 3309, 3243 and 3195 (weak, (w)) ν(N-H)_{dpamH}, 1649(s) δ(N-H)_{dpamH}, 1649(s) ν(C=O), 1601(m) ν(C=N), 1322(sm) ν(C-O→Cd), 837(m), 766(m), 722(m), δ(C-H)_{dpamH}, 523(m) ν(Cd-O); 482(m) ν(Cd-N); UV-vis: λ/nm (ε/M⁻¹cm⁻¹) as nujol

mulls: 368, 427; in DMSO: 370 (3200), 430 (5400); molar conductivity in 1 mM DMSO = 35.0 $\mu\text{S}/\text{cm}$. ^1H -NMR (300 MHz) spectrum in DMSO- d_6 (δ/ppm): 10.10 (1H, s, H^7 5- NO_2 -salo), 8.33 (1H, d, $J = 3.1$ Hz, H^6 5- NO_2 -salo), 8.05 (1H, dd, $J = 9.4$ Hz, 3.1 Hz, H^4 5- NO_2 -salo), 6.69 (1H, d, $J = 9.4$ Hz, H^3 5- NO_2 -salo) and 9.59 (1H, H^7 dpmaH), 8.19 (2H, d, $J = 4.9$ Hz, H^3 and $\text{H}^{3'}$ dpamH), 7.60-7.68 (4H, m, H^5 , $\text{H}^{5'}$, H^6 , $\text{H}^{6'}$ dpamH), 6.84-6.90 (2H, m, H^4 and $\text{H}^{4'}$ dpamH). ^{13}C -NMR (75 MHz) spectrum in DMSO- d_6 (δ/ppm): 191.0, 174.4, 154.3, 147.1, 137.7, 134.3, 129.8, 127.4, 122.6, 122.4, 115.9, 112.1.

[Cd₃(5-NO₂-salo)₆(bipy)₂] (4). The formed yellow crystals suitable for X-ray structure determination, yield 51.0%, 839 mg, analyzed as [Cd₃(5-NO₂-salo)₆(bipy)₂], (C₆₂H₄₀Cd₃N₁₀O₂₄) (MW=1646.14): C, 45.24; H, 2.45; N, 8.51; C, 45.48; H, 2.49; N, 8.53. IR spectrum (KBr): selected peaks in cm^{-1} : 1676, 1647 and (s) $\nu(\text{C}=\text{O})$, 1603(s) $\nu(\text{C}=\text{N})$, 1343(sm) $\nu(\text{C}-\text{O}\rightarrow\text{Cd})$, 833(m), 762(sm), 720(m) $\delta(\text{C}-\text{H})_{\text{pyridyl}}$, 526(m) $\nu(\text{Cd}-\text{O})$, 478(m) $\nu(\text{Cd}-\text{N})$; UV-vis: λ/nm ($\epsilon/\text{M}^{-1}\text{cm}^{-1}$) as nujol mull: 374, 428; in DMSO: 373 (2500), 431 (3100); molar conductivity in 1 mM DMSO = 25.2 $\mu\text{S}/\text{cm}$. ^1H -NMR (300 MHz) spectrum in DMSO- d_6 (δ/ppm): 10.08 (6H, s, H^7 5- NO_2 -salo), 8.28 (6H, d, $J = 3.2$ Hz, H^6 5- NO_2 -salo), 7.89 (6H, dd, $J = 9.6$ Hz, 3.2 Hz, H^4 5- NO_2 -salo), 6.48 (6H, d, $J = 9.6$ Hz, H^3 5- NO_2 -salo) and 8.71 (4H, d, $J = 4.2$ Hz, H^3 - and $\text{H}^{3'}$ -bipy), 8.51 (4H, d, $J = 8.0$ Hz, H^6 - and $\text{H}^{6'}$ -bipy), 8.11 (4H, dd as t, $J = 7.6$ Hz, H^5 - and $\text{H}^{5'}$ -bipy), 7.62 (4H, dd as t, $J = 6.1$ Hz, H^4 - and $\text{H}^{4'}$ -bipy). ^{13}C -NMR (75 MHz) spectrum in DMSO- d_6 (δ/ppm): 192.1, 179.4, 151.8, 149.2, 139.1, 131.4, 129.3, 128.6, 125.4, 124.9, 122.4, 121.7.

[Cd(5-NO₂-salo)(neoc)(NO₃)₂] (5). Yellow solid, yield 50.0%, 549 mg, analyzed as [Cd(5-NO₂-salo)(neoc)(NO₃)₂], (C₄₂H₃₂Cd₂N₈O₁₄) (MW=1097.58): C, 45.96; H, 2.94; N, 10.21. Found: C, 45.91; H, 2.95; N, 10.11. IR spectrum (KBr): selected peaks in cm^{-1} : 1652(s) $\nu(\text{C}=\text{O})$, 1597(m) $\nu(\text{C}=\text{N})$, 1315(sm) $\nu(\text{C}-\text{O}\rightarrow\text{Cd})$, 860(m), 761(m) and 730(sm) $\delta(\text{C}-\text{H})_{\text{neoc}}$, 550(m) $\nu(\text{Cd}-\text{O})$; 476(m) $\nu(\text{Cd}-\text{N})$; UV-vis: λ/nm ($\epsilon/\text{M}^{-1}\text{cm}^{-1}$) as nujol mulls: 370, 428; in DMSO: 373 (2700), 431 (4730); molar conductivity in 1 mM DMSO = 24.7 $\mu\text{S}/\text{cm}$. ^1H -NMR (300 MHz) spectrum in DMSO- d_6 (δ/ppm): 9.78 (1H, s, H^7 5- NO_2 -salo), 8.30 (1H, d, $J = 3.1$ Hz, H^6 5- NO_2 -salo), 7.93-7.87 (3H, m, overlapped H^4 5- NO_2 -salo and H^3 H^8 neoc), 6.45 (1H d, $J = 9.6$ Hz, 5- NO_2 -salo) and 8.64 (2H, d, $J = 8.3$ Hz, H^4 and H^7 neoc), 8.07 (2H, s, H^5 and H^6 neoc), 2.98 (6H, s, CH₃ neoc). ^{13}C -NMR (75 MHz) spectrum in DMSO- d_6 (δ/ppm): 193.6, 178.7, 159.8, 140.6, 139.2, 132.3, 130.1, 129.6, 127.1, 126.0, 125.7, 124.8, 122.0, 25.0.

2.3. X-ray crystal structure determination

Single crystals of $[\text{Cd}(5\text{-NO}_2\text{-salO})_2(\text{CH}_3\text{OH})_2]$ (**1**), $[\text{Cd}(5\text{-NO}_2\text{-salO})_2(\text{phen})]\cdot 2\text{CH}_3\text{OH}\cdot \text{H}_2\text{O}$ (**2**), $[\text{Cd}(5\text{-NO}_2\text{-salO})_2(\text{dpamH})]$ (**3**) and $[\text{Cd}_3(5\text{-NO}_2\text{-salO})_6(\text{bipy})_2]$ (**4**), suitable for crystal structure analysis, were obtained by slow evaporation of their mother liquids at room temperature. They were mounted at room temperature on a Bruker Kappa APEX2 diffractometer equipped with a triumph monochromator using Mo $K\alpha$ radiation. Unit cell dimensions were determined and refined by using the angular settings of at least 200 high intensity reflections ($>10 \sigma(I)$) in the range $11 < 2\theta < 36^\circ$. Intensity data were recorded using ϕ and ω scans. All crystals presented no decay during the data collection. The frames collected for each crystal were integrated with the Bruker SAINT Software package [39] using a narrow-frame algorithm. Data were corrected for absorption using the numerical method (SADABS) based on crystal dimensions [40]. All structures were solved using the SUPERFLIP package [41], incorporated in Crystals. Data refinement (full-matrix least-squares methods on F^2) and all subsequent calculations were carried out using the Crystals version 14.40b program package [42]. All non-hydrogen atoms were refined anisotropically. Hydrogens were located by difference maps at their expected positions and refined using soft constraints. By the end of the refinement, they were positioned geometrically using riding constraints to bonded atoms. Illustrations with 50% ellipsoids probability were drawn by CAMERON [43]. Crystal data for **1-4** are provided in table 1.

2.4. DNA-binding studies

In order to study the interaction of DNA with **1-5**, the compounds were initially dissolved in DMSO (1 mM). Mixing of such solutions with the aqueous buffer DNA solutions used in the studies never exceeded 5% DMSO (v/v) in the final solution, which was needed due to low aqueous solubility of most compounds. All studies were performed at room temperature. The interaction of free 5-NO₂-salOH with CT DNA was recently reported [32].

Study with UV spectroscopy. The interaction of **1-5** with CT DNA was studied by UV spectroscopy in order to investigate the possible binding modes to CT DNA and to calculate the binding constants to CT DNA (K_b). Control experiments with 5% DMSO were performed and no changes in the spectra of CT DNA were observed. The UV spectra of CT DNA in the presence of each compound were recorded for a constant CT DNA concentration in diverse mixing ratios

($r = [\text{compound}]/[\text{DNA}]$). The binding constant of the compounds with DNA, K_b (in M^{-1}), were determined by the Wolfe–Shimer equation (eq. S1) [44] and the plots $\frac{[\text{DNA}]}{(\epsilon_A - \epsilon_f)}$ vs $[\text{DNA}]$ using the UV spectra of the compounds recorded, for a constant concentration in the presence of DNA at diverse ratios ($r' = [\text{DNA}]/[\text{compound}]$).

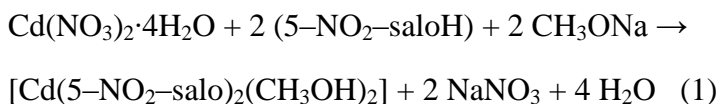
Viscometry. Viscosity experiments were carried out using an ALPHA L Fungilab rotational viscometer equipped with an 18 mL LCP spindle and the measurements were performed at 100 rpm. The viscosity of DNA ($[\text{DNA}] = 0.1 \text{ mM}$) in buffer solution (150 mM NaCl and 15 mM trisodium citrate at pH 7.0) was measured in the presence of increasing amounts of **1-5** up to $r = 0.35$. All measurements were performed at room temperature. The obtained data are presented as $(\eta/\eta_0)^{1/3}$ versus r , where η is the viscosity of DNA in the presence of the compound and η_0 is the viscosity of DNA alone in buffer solution.

EB competitive studies with fluorescence spectroscopy. Competitive studies of each compound with EB were investigated with fluorescence spectroscopy in order to examine whether the compound can displace EB from its DNA–EB complex. The DNA–EB complex was prepared by adding 20 μM EB and 26 μM CT DNA in buffer (150 mM NaCl and 15 mM trisodium citrate at pH 7.0). The possible intercalating effect of the compounds (5–NO₂–saloH and **1-5**) was studied by adding a certain amount of a solution of the compound step by step into a solution of the pre-treated DNA–EB complex. The influence of the addition of each compound to the DNA–EB complex solution has been obtained by recording the variation of fluorescence emission spectra with excitation wavelength at 540 nm. The compounds do not show any fluorescence emission at room temperature in solution or in the presence of DNA under the same experimental conditions; therefore, the observed quenching is attributed to the displacement of EB from its EB–DNA complex. The values of the Stern–Volmer constant (K_{SV} , in M^{-1}) have been calculated according to the linear Stern–Volmer equation (eq. S2) [45, 46] and the corresponding plots.

3. Results and discussion

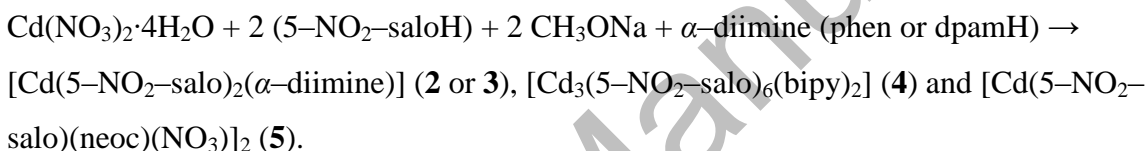
3.1. Synthesis–general considerations of the complexes

The reaction of $\text{Cd}(\text{NO}_3)_2 \cdot 4\text{H}_2\text{O}$ with deprotonated 5–NO₂–saloH in methanol afforded solid microcrystalline compound in good yield, according to reaction (1).



The resultant cadmium(II) complex $[\text{Cd}(5\text{-NO}_2\text{-salO})_2(\text{CH}_3\text{OH})_2]$ (**1**) is neutral (molar conductivity in DMSO solution was $15.0 \mu\text{S}\cdot\text{cm}^{-1}$) and possesses a 1:2 metal-to-ligand composition, as it is indicated from elemental analysis. It is soluble in CH_3OH , DMF and DMSO, but not in CH_3CN , CH_3COCH_3 , CH_2Cl_2 , EtOH, H_2O and Et_2O .

The reaction of methanolic solutions of $\text{Cd}(\text{NO}_3)_2 \cdot 4\text{H}_2\text{O}$, 5- NO_2 -salOH and an α -diimine (bipy, phen, neoc, dpamH) led to complexes **2-5**, respectively, with three different formulas and coordination modes of 5- NO_2 -salO⁻, depending on the α -diimine used, as following:



The synthesized cadmium(II) complexes are neutral, soluble in DMF and DMSO, but insoluble in most organic solvents and H_2O . Evidence of the coordination mode of the ligands in the cadmium compounds has also arisen from the interpretation of the IR, UV, ^1H - and ^{13}C -NMR data of the 5-nitro-salicylaldehyde, the α -diimines and the complexes. In these compounds, the α -diimine is coordinated as a neutral bidentate ligand through the heterocyclic nitrogens, while 5-nitro-salicylaldehyde behaves as a monoanionic ligand, coordinated to cadmium ion through the phenolato oxygen in all complexes, but bidentate and/or tridentate in different complexes, as will be clarified by spectroscopy and X-ray crystallography.

3.2. Spectroscopy (IR, UV-vis, ^1H - and ^{13}C -NMR)

IR spectroscopy was used to confirm the deprotonation and the binding mode of 5- NO_2 -salOH as well as the binding modes of the α -diimines. In the IR spectra of the complexes, the peaks of the stretching and bending vibrational modes of the phenolic OH of 5- NO_2 -salOH found around 3200 cm^{-1} and 1400 cm^{-1} in the IR spectrum of free 5- NO_2 -salOH, respectively, disappear indicating deprotonation of the salicylaldehyde [47, 48]. Additionally, the peak originating from

the C–O stretching vibration at 1276 cm⁻¹ in the complexes exhibits positive shifts to ~1300 cm⁻¹ denoting coordination through the deprotonated phenolic oxygen.

The peak at ~1660 cm⁻¹, attributable to the aldehyde bond $\nu(\text{HC}=\text{O})$ of the free 5-NO₂-salOH, is shifted to lower frequencies (~1630 cm⁻¹) in the complexes, thus denoting the bidentate mono-anionic character of the ligand [49]. This is valid for **1**, **4** and **5**. However, for **2** and **3** with bipy and phen, respectively, besides the peak at 1630 cm⁻¹, there is an additional peak at ~1660 cm⁻¹, which denotes the presence of non-coordinated aldehyde oxygen of salicylaldehyde ligand in these complexes.

The intense bands at ~1590 cm⁻¹ attributed to the stretching vibrations $\nu(\text{C}=\text{N})_{\text{aromatic}}$ are present in the mixed-ligand complexes, denoting coordination through the nitrogens of the α -diimine ligands. The IR spectrum of **5** demonstrates also the presence of coordinated nitrates. Two strong bands at 1488–1502 cm⁻¹ and 1288–1302 cm⁻¹, assigned to the ν_4 and ν_1 vibrations of nitrate, respectively (C_{2v} symmetry, coordinated nitrate). The magnitude of the splitting Δ , where $\Delta = \nu_4 - \nu_1$, is ~136 cm⁻¹ and it is typical of monodentate (M–O–NO₂) bonding of nitrates [50].

¹H-NMR spectroscopy was also used in order to confirm deprotonation of the salicylaldehyde and the stability of the complexes in solution. The deprotonation of the phenolic hydrogen can be easily concluded from the absence of the –OH signal, which is observed in the ¹H-NMR spectra of the free 5-NO₂-salOH, appearing as single peak at $\delta = 12$ ppm. The ¹H-NMR spectra of **1-5** are consistent with the obtained structures. All the expected signals related to the presence of the ligands in the corresponding compounds are present; four signals for the 5-NO₂-salO and four for the α -diimine ligands, as shown representatively for **2** and **4** in figure 1. From the number of protons in the ¹H-NMR spectra of the complexes, we conclude that the ratio of 5-NO₂-salicylaldehyde to α -diimine is 2:1 in **2** and **3**, 3:1 in **4** and 1:1 in **5**. All signals are slightly shifted as expected upon binding to cadmium ion. The ¹H-NMR spectra of the complexes give the protons, attributable to the aldehyde group at δ 9.78-10.10 ppm.

¹³C-NMR spectra give also the expected sets of chemical shifts for both the 5-NO₂-salO and the diimine moieties; seven peaks for 5-NO₂-salO⁻ and five or six for the diimine. The most characteristic peaks are that of carbonyl carbon at δ 193.6-191.0 ppm and C-2 of 5-NO₂-salO at $\delta = 179.4$ -174.4 ppm. The absence of additional set of signals related to dissociated ligands suggests that all complexes remain intact in solution.

The UV spectra of the complexes were recorded as nujol mull and in DMSO solution and are similar, suggesting that the complexes retain their structure in solution. In addition, the UV spectra of the complexes were also recorded in the series of pH (pH range 6–8, since the biological experiments are performed at pH = 7) with the use of diverse buffer solutions (150 mM NaCl and 15 mM trisodium citrate at pH values regulated by HCl solution) so as to explore the stability of complexes in buffer solution; no significant changes (shift of the λ_{max} or new peaks) were observed in the spectra of **1-5**, indicating that they may keep their integrity in the pH range 6–8 [51, 52].

The fact that the complexes are non-electrolytes in DMSO solution ($\Lambda_{\text{M}} = 15\text{--}35 \text{ mho cm}^2 \text{ mol}^{-1}$, in 1 mM DMSO solution) having similar UV spectral patterns in nujol, in DMSO solution and in the presence of the buffer solution and that their $^1\text{H-NMR}$ spectra confirm no dissociation, may suggest that the compounds are stable in DMSO solution [53].

3.3. Description of the structures

The molecular structures of **1-4** with the atom numbering scheme are shown in figures 2-4, respectively, and selected bond distances and angles are given in table 2.

3.3.1. Description of the structure of $[\text{Cd}(5\text{-NO}_2\text{-salO})_2(\text{CH}_3\text{OH})_2]$ (1**).** In the molecular structure of $[\text{Cd}(5\text{-NO}_2\text{-salO})_2(\text{CH}_3\text{OH})_2]$ (**1**), two 5-NO₂-salicylaldehyde anions are chelated through the phenolate oxygen (O1) and the carbonyl (O2) to the cadmium cation in *trans*-positions and occupy the equatorial plane. In **1**, as well as in **2** and **3**, the Cd–(O1) (phenolic oxygen) distance is shorter than the Cd–(O2) (carbonyl oxygen) distance, as expected, suggesting stronger coordination ability of the ionic phenolate oxygen (table 2). A slightly distorted octahedral coordination is achieved by binding of two methanol molecules in the axial positions (figure 2). The mean planes of the two salicylaldehyde ligands in the same complex are parallel but not co-planar having a distance of 1.574 Å. The Cd(II) ion is situated in the mid distance due to symmetry reasons. Strong intermolecular hydrogen bonding interactions arise from the methanol hydroxyl groups to the phenolate O forming chains of complex planes parallel to 'a' crystallographic axis. Bond distances of coordinated 5-NO₂-salicylaldehyde are similar to a reported mixed-ligand 5-NO₂-salicylaldehydato copper(II) complex [54].

3.3.2. Description of the structures of [Cd(5-NO₂-salo)₂(α -diimine)] (2 and 3, phen and dpamH, respectively). The complexes [Cd(5-NO₂-salo)₂(phen)]·2CH₃OH·H₂O (**2**) and [Cd(5-NO₂-salo)₂(dpamH)] (**3**) have similar structures. One phenanthroline (phen) or dipyridylamine (dpamH) is coordinated in a bidentate manner (through two pyridine nitrogens as a neutral ligand) forming a five-membered chelate ring with the cadmium ion, while two 5-NO₂-salo monoanionic ligands are coordinated to the cadmium cation in a chelating bidentate way (through the deprotonated phenolic and the carbonyl oxygen atoms), forming a six-membered ring (figure 3). The cadmium ion is six-coordinate and its geometry octahedral with a CdO₄N₂ chromophore. The structure of **3** is stabilized by N_{am}H...O_{phenolic} type hydrogen-bonds between two neighboring complex molecules forming complex dimers. Hydrogen-bonding in **2** arises only between methanol and water molecules.

3.3.3. Description of the structure of [Cd₃(5-NO₂-salo)₆(bipy)₂] (4). In [Cd₃(5-NO₂-salo)₆(bipy)₂] (**4**), the six deprotonated 5-NO₂-salo⁻ ligands are coordinated in three different modes: (i) as a bidentate ligand bridging two cadmium cations Cd1 and Cd2 through only the phenolic O9, (ii) as a bidentate chelating anion through the phenolic O1 and the aldehyde O2 bounded to the terminal cadmium cations Cd1 and (iii) as a tridentate ligand, *i.e.* chelating the central cadmium Cd2 through the phenolic O5 and the aldehyde O6 and bridging via O5 to central and one terminal cadmium Cd1. To the best of our knowledge, this is the first time that such combination of coordination modes of the same substituted salicylaldehyde in the same compound is reported. The average Cd-O_{phenolic} distance is comparable to those found in other trinuclear cadmium complexes with Schiff bases [55]. The central cadmium ion has a CdO₆ chromophore and octahedral geometry. The four coordinated oxygens are monodentate bridging phenolic oxygens and aldehyde oxygens. The two terminal cadmium cations are six-coordinate having a distorted octahedral geometry. Besides the four oxygens from 5-NO₂-salo⁻ ligands (one is aldehyde, one monodentate phenolic and two bridging phenolic), their coordination sphere is completed by two nitrogens (N4 and N5) from the bipy ligands giving a CdO₄N₂ chromophore. The Cd-N distances are within the expected limits [56]. The distance between the two cadmium ions is Cd1...Cd2 = 3.588(5) Å.

3.4. Thermal investigation

The thermal stabilities and decomposition modes of **1-3** were investigated by the simultaneous TG/DTG/DTA technique, in nitrogen atmosphere with heating rate $10\text{ }^{\circ}\text{C min}^{-1}$, from ambient to $900\text{ }^{\circ}\text{C}$. The profiles of their thermoanalytical curves reveal complicated decomposition, in connection with the release of the ligand molecules, as depicted in figure 5 for **1** and **2**. The release of coordinated methanol in **1** or crystallized methanol in **2** takes place first in both compounds. Then follows the decomposition of the ligand and finally for **2** the decomposition of 1,10-phenanthroline. In both cases the residue at $900\text{ }^{\circ}\text{C}$ consists of a mixture of carbonaceous metal along with cadmium oxide CdO.

3.5. Interaction with calf-thymus DNA

The interaction of transition metal complexes with DNA mainly depends on the structure and the nature of the coordinated ligands. Thus, transition metal complexes may interact with double-stranded DNA via: (i) covalent bonding, via the replacement of one or more labile ligands by a nitrogen base of DNA, (ii) non-covalent mode, *i.e.* (a) intercalation of the complex between DNA nucleobases via $\pi\rightarrow\pi$ stacking interactions, (b) electrostatic interactions between metal complexes and the phosphate groups of DNA when Coulomb forces may develop, and (c) groove-binding due to the presence of van der Waals forces or hydrogen-bonding or hydrophobic bonding along the major or minor groove of the DNA helix, and (iii) cleavage of the DNA helix along and/or across its length [57].

3.5.1. UV spectroscopy and DNA-interaction. UV-Vis spectroscopy is a useful tool to provide information in regard to mode and strength of binding of compounds with DNA. The existence of any interaction between the compound and CT DNA will perturb the band of CT DNA at 258–260 nm or the intra-ligand transition bands of the compound, respectively, during the titrations. Red-shift shows stabilization of the structure because of the interaction; blue-shift is evidence of structural destabilization. Furthermore, the intense hypochromism of a transition band, which is usually accompanied by bathochromism, is clear evidence of an intercalative binding mode [58]. In particular, the UV spectra of a CT DNA solution ($1.0\text{--}1.5 \times 10^{-4}\text{ M}$) were recorded in the presence of **1-5** at increasing amounts (for different *r* values) as well as the UV

spectra of DMSO solution (1×10^{-5} – 5×10^{-5} M) of **1-5** in the presence of CT DNA at increasing amounts of r' .

The UV spectra of DNA solution were recorded in the presence of **1-5** at increasing r values (up to 0.3). The UV spectra of the DNA solution in the presence of **1-5** are quite similar exhibiting slight hypochromism of the DNA band at 258 nm, which may be considered as evidence of the formation of a new adduct of the compound with double-helical DNA resulting in stabilization of the DNA duplex [58]. The UV spectra of DNA solution in the presence of **2** at diverse r values are shown in figure 6(A).

Additionally, the UV spectra of **1-5** in DMSO (1×10^{-5} – 5×10^{-5} M) were recorded in the presence of CT DNA at increasing amounts. In the UV spectra of **2** (figure 6(B)), the two observed bands at 373 nm (band I) and 432 nm (band II) exhibit in the presence of increasing amounts of CT DNA a slight ($\sim 1\%$) and a more intense hypochromism ($\sim 12.5\%$), respectively, followed by blue-shift of up to 7 nm. Quite similar is the behavior of **1** and **3-5** in the presence of CT DNA which in most cases exhibit a higher hypochromism (table 3).

It is quite evident that conclusions concerning the DNA-binding mode of the compounds cannot be safely drawn only by UV spectroscopic studies and more techniques should be combined. The data derived by the UV titration experiments suggest that all compounds can bind to CT DNA, while the observed hypochromism might infer the existence of intercalation [58].

The magnitude of the binding strength for a compound with CT DNA may be evaluated through calculation of the DNA-binding constant (K_b). The K_b values were obtained by plots

$\frac{[\text{DNA}]}{(\epsilon_A - \epsilon_f)}$ versus [DNA] (figure S1) using the Wolfe-Shimer equation [44]. The K_b values of

1-5 (table 3) are relatively high suggesting tight binding of the complexes to CT DNA, with **3** having the highest K_b value ($1.65(\pm 0.10) \times 10^6 \text{ M}^{-1}$) among the complexes, and are of similar magnitude to that of the classical intercalator EB ($1.23(\pm 0.07) \times 10^5 \text{ M}^{-1}$) [59]. Complexes **1-5** have higher K_b values than their Zn analogues with 5- NO_2 -sal $^-$ ligands [32] and are significantly higher than a series of Cd complexes found in the literature [12-18].

3.5.2. DNA-binding study with viscosity measurements. The viscosity of DNA (η) is sensitive to DNA length changes since the relation between the relative DNA-solution viscosity (η/η_0) and DNA length (L/L_0) is given by the equation $(L/L_0) = (\eta/\eta_0)^{1/3}$, where L_0 and L denote the apparent

molecular length in the absence and presence of a compound, respectively [60, 61]. This characteristic is helpful when investigating the interaction of a compound with DNA. Intercalation (insertion of the compound in between the DNA base pairs) will result in an increase of the separation distance of base pairs lying at intercalation sites, causing an increase of the DNA-helix length which will result in an increase of DNA viscosity; the magnitude of which is usually in accord to the strength of the interaction. When a compound binds to DNA grooves via a partial or non-classic intercalation (*i.e.* electrostatic interaction or external groove-binding), a bend or kink in the DNA-helix may result in slight shortening of its effective length; in this case, the change in viscosity of the DNA solution is less pronounced or there is no change at all [60-62].

DNA-viscosity measurements were carried out on CT DNA solutions (0.1 mM) upon addition of increasing amounts of the compounds (up to the value of $r = 0.35$) at room temperature. The relative viscosity of DNA solution exhibits an increase upon addition of **1-5** which is more significant than that of free 5-NO₂-salOH (figure 7). The behavior of the DNA viscosity observed upon addition of the compounds may be considered evidence of the existence of an intercalative binding mode to DNA, a conclusion which clarifies the findings from the UV spectroscopic titrations.

3.5.3. EB-displacement studies. The excitation of a solution containing EB and DNA at $\lambda_{\text{excitation}} = 540$ nm (as EB-DNA compound) results in an intense fluorescence emission band at ~ 592 nm. This is due to the intercalation of the planar EB phenanthridine ring between adjacent DNA-base pairs, since EB is a typical DNA-intercalator. When a compound which has equal or higher intercalative ability towards DNA than EB is added into this solution, a significant quenching of the EB-DNA fluorescence emission may be induced. Complexes **1-5** do not show any fluorescence emission at room temperature in solution or in the presence of CT DNA under the same experimental conditions, *i.e.* $\lambda_{\text{exc}} = 540$ nm. The addition of the complexes into an EB solution does not quench the EB fluorescence emission and does not result in the appearance of new peaks in the spectra. Therefore, the changes observed in the fluorescence emission spectra of the EB-DNA solution, when the complexes are added, may be useful to examine the EB-displacing ability of the complexes, mainly as indirect evidence and verification of their intercalating ability.

The fluorescence emission spectra of pre-treated EB–DNA ($[EB] = 20 \mu\text{M}$, $[DNA] = 26 \mu\text{M}$) were recorded in the presence of increasing amounts of **1-5** up to the value of $r = 0.17$ (representatively shown for **1** in figure 8(A)). The addition of the complexes results in a significant quenching (up to 62.4–86.7%, table 4) of the initial EB–DNA fluorescence emission band at 592 nm (figure 8(B)), indicating significant EB–displacing ability of the complexes and, thus, revealing indirectly the interaction with CT DNA by intercalation [45].

The Stern–Volmer plots (figure S2) illustrate that the observed EB–DNA fluorescence emission quenching was in agreement ($R = 0.99$) with the linear Stern–Volmer equation (eq. S2); therefore, the observed quenching is a result of the displacement of EB from EB–DNA by each complex [32, 33]. The K_{SV} values (table 4) of the complexes calculated by the Stern–Volmer equation using the Stern–Volmer plots are relatively high and suggest tight binding to DNA. In particular, the K_{SV} values of most complexes are higher than that of free 5–NO₂–salOH, with **1** possessing the highest K_{SV} value ($1.41(\pm 0.03) \times 10^6 \text{ M}^{-1}$) among the complexes. Additionally, the K_{SV} values of **1-5** are higher than those of their Zn analogues [32].

4. Conclusion

The synthesis and characterization of cadmium complexes with 5–nitro–salicylaldehyde in the absence or presence of an α –diimine (bipy, phen, neoc or dpamH) has been achieved. The reaction of $\text{Cd}(\text{NO}_3)_2 \cdot 4\text{H}_2\text{O}$ and deprotonated 5–NO₂–salicylaldehyde under aerobic conditions resulted in formation of $[\text{Cd}(5\text{–NO}_2\text{–salO})_2(\text{CH}_3\text{OH})_2]$ (**1**), while the addition of the α –diimine (phen or dpamH) led to the formation of $[\text{Cd}(5\text{–NO}_2\text{–salO})_2(\alpha\text{–diimine})]$ (**2** or **3**), the trimeric $[\text{Cd}_3(5\text{–NO}_2\text{–salO})_6(\text{bipy})_2]$ (**4**), and the dimeric $[\text{Cd}(5\text{–NO}_2\text{–salO})(\text{neoc})(\text{NO}_3)]_2$ (**5**), as shown by spectroscopy (IR, UV–Vis and NMR), and proved by X-ray crystallography for **1-4**, providing confirmation of different coordination modes. The thermal stability of **1-3** showed the complicated nature of their thermal decomposition in nitrogen.

The interaction of **1-5** with CT DNA was explored with several techniques. UV spectroscopic studies revealed the ability of the complexes to bind to CT DNA. The complexes can bind tightly to DNA as estimated by the DNA–binding constants (K_b) with $[\text{Cd}(5\text{–NO}_2\text{–salO})_2(\text{dpamH})]$ (**3**), showing the highest K_b value ($1.65 \times 10^6 \text{ M}^{-1}$) among the complexes. DNA viscosity measurements revealed that the probable DNA-binding mode of the complexes is

intercalation, a conclusion which was also verified by the significant ability of the complexes to displace the classical intercalator EB from its EB–DNA compound.

Appendix A. Supplementary material

The crystal structures of **1**, **2**, **3** and **4** have been submitted to the CCDC and have been allocated the deposition numbers CCDC 1055222-1055225, respectively. These data can be obtained free of charge via www.ccdc.cam.ac.uk/conts/retrieving.html (or from the Cambridge Crystallographic Data Centre, 12 Union Road, Cambridge CB21EZ, UK; Fax: (+44) 1223-336-033; or deposit@ccdc.cam.ac.uk). Supplementary data associated with this article can be found in the online version.

Acknowledgements

This work was funded by Aristeia 2014, Aristotle University of Thessaloniki.

References

- [1] P. Joseph. *Toxicol. Appl. Pharmacol.*, **238**, 272 (2009).
- [2] D.M. Templeton, Y. Liu. *Chem. Biol. Interact.*, **188**, 267 (2010).
- [3] T.G. Kho, M.K. Break, K.A. Crouse, M. Ibrahim, M. Tahir, A.M. Ali, A.R. Cowley, D.J. Watkin, M.T.H. Tarafder. *Inorg. Chim. Acta*, **413**, 68 (2014).
- [4] M. Montazerzohori, S. Musavi, A. Masoudiasl, A. Naghiha, M. Dusek, M. Kucerakova. *Spectrochim. Acta, Part A*, **137**, 389 (2015).
- [5] M. Montazerzohori, S. Zahedi, M. Nasr–Esfahani, A. Naghiha. *J. Ind. Eng. Chem.*, **20**, 2463 (2014).
- [6] N.R. Filipovic, A. Bacchi, M. Lazic, G. Pelizzi, S. Radulovic, D.M. Sladic, T.R. Todorovic, K.K. Anelkovic. *Inorg. Chem. Commun.*, **11**, 47 (2008).
- [7] S. Bjelogrljic, T. Todorovic, A. Bacchi, M. Zec, D. Sladic, T. Srdic–Rajic, D. Radanovic, S. Radulovic, G. Pelizzi, K. Andjelkovic. *J. Inorg. Biochem.*, **104**, 673 (2010).
- [8] R. Chen, C. Liu, H. Zhang, Y. Guo, X. Bu, M. Yang. *J. Inorg. Biochem.*, **101**, 412 (2007).
- [9] C. Ma, S. Liang, F. Zhao, Y. Meng, Y. Li, M. Zhu, E. Gao. *J. Coord. Chem.*, **67**, 3551 (2014).

- [10] D. Hall, R. Holmlin, J.K. Barton. *Nature*, **382**, 731 (1996).
- [11] X. Yang, J. Feng, J. Zhang, Z. Zhang, H. Lin, L. Zhou, X. Yu. *Bioorg. Med. Chem.*, **16**, 3871 (2008).
- [12] H. Wu, J. Yuan, X. Huang, F. Kou, B. Liu, F. Jia, K. Wang, Y. Bai. *Inorg. Chim. Acta*, **390**, 12 (2012).
- [13] J. Lu, Q. Su, J. Li, W. Gu, J. Tian, X. Liu, S. Yan. *J. Coord. Chem.*, **66**, 3280 (2013).
- [14] N.A. Illan-Cabeza, R.A. Vilaplana, Y. Alvarez, K. Akdi, S. Kamah, F. Hueso-Urena, M. Quiros, F. Gonzalez-Vilchez, M.N. Moreno-Carretero. *J. Biol. Inorg. Chem.*, **10**, 924 (2005).
- [15] H. Park, J.H. Kwon, T. Cho, J.M. Kim, I.H. Hwang, C. Kim, S. Kim, J. Kim, S.K. Kim. *J. Inorg. Biochem.*, **127**, 46 (2013).
- [16] H.-L. Wu, K.-T. Wang, F. Kou, F. Jia, B. Liu, J.-K. Yuan, Y. Bai. *J. Coord. Chem.*, **64**, 2676 (2011).
- [17] C. Gao, X. Ma, J. Tian, D. Li, S. Yan. *J. Coord. Chem.*, **63**, 115 (2010).
- [18] H.-L. Wu, K. Wang, F. Jia, B. Liu, F. Kou, J. Yuan, J. Kong. *J. Coord. Chem.*, **63**, 4113 (2010).
- [19] R.N. Prasad, A. Agrawal. *J. Ind. Chem. Soc.*, **83**, 75 (2006).
- [20] R.N. Prasad, M. Agrawal, R. George. *J. Ind. Chem. Soc.*, **82**, 444 (2005).
- [21] S.T. Hussain, H. Ahmad, M.A. Atta, M. Afzal, M. Saleem. *J. Trace Microprobe Tech.*, **16**, 139 (1998).
- [22] K. Fujinaga, Y. Sakaguchi, T. Tsuruhara, Y. Seike, M. Okumura. *Solvent Extract. Res. Develop.*, **8**, 144 (2001).
- [23] E. Pelttari, E. Karhumaki, J. Langshaw, H. Perakyla, H. Elo. *Z. Naturforsch.*, **62c**, 487 (2007).
- [24] A. Jayamani, N. Sengottuvelan, G. Chakkaravarthi. *Polyhedron*, **81**, 764 (2014).
- [25] Y. Yang, P. Lu, T. Zhu, C. Liu. *Acta Cryst.*, **E63**, m1613 (2007).
- [26] Q. Wang, D. Wang. *Acta Cryst.*, **E64**, m298 (2008).
- [27] J.C Pessoa, I. Cavaco, I. Correira, I. Tomaz, T. Duarte, P. Matias. *J. Inorg. Biochem.*, **80**, 35 (2000).
- [28] M. Lalia-Kantouri, C.D. Papadopoulos, A.G. Hatzidimitriou, M.P. Sigalas, M. Quiros, S. Skoulika. *Polyhedron*, **52**, 1306 (2013).

- [29] M. Lalia-Kantouri, T. Dimitriadis, C.D. Papadopoulos, M. Gdaniec, A. Czapik, A.G. Hatzidimitriou. *Z. Anorg. Allg. Chem.*, **635**, 2185 (2009).
- [30] C.D. Papadopoulos, A.G. Hatzidimitriou, M. Quiros, M.P. Sigalas, M. Lalia-Kantouri. *Polyhedron*, **30**, 486 (2011).
- [31] M. Lalia-Kantouri, M. Gdaniec, T. Choli-Papadopoulou, A. Badounas, C.D. Papadopoulos, A. Czapik, G.D. Geromichalos, D. Sahpazidou, F. Tsitouroudi. *J. Inorg. Biochem.*, **117**, 25 (2012).
- [32] A. Zianna, G. Psomas, A. Hatzidimitriou, E. Coutouli-Argyropoulou, M. Lalia-Kantouri. *J. Inorg. Biochem.*, **127**, 116 (2013).
- [33] E. Mrkalic, A. Zianna, G. Psomas, M. Gdaniec, A. Czapik, E. Coutouli-Argyropoulou, M. Lalia-Kantouri. *J. Inorg. Biochem.*, **134**, 66 (2014).
- [34] A. Zianna, K. Chrissafis, A. Hatzidimitriou, M. Lalia-Kantouri. *J. Therm. Anal. Calorim.*, **120**, 59 (2015).
- [35] A. Zianna, G. Psomas, A. Hatzidimitriou, M. Lalia-Kantouri. *RSC Adv.*, **5**, 37495 (2015).
- [36] J. Marmur. *J. Mol. Biol.*, **3**, 208 (1961).
- [37] M.F. Reichmann, S.A. Rice, C.A. Thomas, P. Doty. *J. Am. Chem. Soc.*, **76**, 3047 (1954).
- [38] A. Zianna, S. Vecchio, M. Gdaniec, A. Czapik, A. Hatzidimitriou, M. Lalia-Kantouri. *J. Therm. Anal. Calorim.*, **112**, 455 (2013).
- [39] Bruker Analytical X-ray Systems, Inc. Apex2, Version 2 User Manual, M86-E01078, Madison, WI (2006).
- [40] Siemens Industrial Automation, Inc. *SADABS: Area-Detector Absorption Correction*, Madison, WI (1996).
- [41] L. Palatinus, G. Chapuis. *J. Appl. Cryst.*, **40**, 786 (2007).
- [42] P.W. Betteridge, J.R. Carruthers, R.I. Cooper, K. Prout, D.J. Watkin. *J. Appl. Cryst.*, **36**, 1487 (2003).
- [43] D.J. Watkin, C.K. Prout, L.J. Pearce, *CAMERON Program, Chemical Crystallographic Laboratory*, Oxford University, UK (1996).
- [44] A. Wolfe, G. Shimer, T. Meehan. *Biochemistry*, **26**, 6392 (1987).
- [45] G. Zhao, H. Lin, S. Zhu, H. Sun, Y. Chen. *J. Inorg. Biochem.*, **70**, 219 (1998).

- [46] J.R. Lakowicz, *Principles of Fluorescence Spectroscopy*, 3rd Edn., Plenum Press, New York (2006).
- [47] R.M. Silverstein, G.C. Bassler, G. Morvill, *Spectrometric Identification of Organic Compounds*, 6th Edn., Wiley, New York (1998).
- [48] K. Nakamoto, *Infrared and Raman Spectra of Inorganic and Coordination Compounds, Part B: Applications in Coordination, Organometallic, and Bioinorganic Chemistry*, 6th Edn., Wiley, New Jersey (2009).
- [49] A. Tarushi, C.P. Raptopoulou, V. Psycharis, A. Terzis, G. Psomas, D.P. Kessissoglou. *Bioorg. Med. Chem.*, **18**, 2678 (2010).
- [50] K. Nakamoto, *Infrared and Raman Spectra of Inorganic and Coordination Compounds*, 4th Edn., Wiley-Interscience, New York, 254 (1986).
- [51] F. Dimiza, A.N. Papadopoulos, V. Tangoulis, V. Psycharis, C.P. Raptopoulou, D.P. Kessissoglou, G. Psomas. *J. Inorg. Biochem.*, **107**, 54 (2012).
- [52] A. Tarushi, F. Kastanias, V. Psycharis, C.P. Raptopoulou, G. Psomas, D.P. Kessissoglou. *Inorg. Chem.*, **51**, 7460 (2012).
- [53] A. Tarushi, K. Lafazanis, J. Kljun, I. Turel, A.A. Pantazaki, G. Psomas, D.P. Kessissoglou. *J. Inorg. Biochem.*, **121**, 53 (2013).
- [54] Y.M. Chumakov, L.G. Paladi, B.Y. Antosyak, Y.A. Simonov, V.I. Tsapkov, G. Bocelli, A.P. Gulea, D. Ginju, S.A. Palomares–Sanchez. *Crystallogr. Rep.*, **56**, 260 (2011).
- [55] K. Agapiou, M.L. Mejia, X. Yang, B.J. Holliday. *Dalton Trans.*, 4154 (2009).
- [56] X. Tai, J. Jiang. *Materials*, **5**, 1626 (2012).
- [57] B.M. Zeglis, V.C. Pierre, J.K. Barton. *Chem. Commun.*, 4565 (2007).
- [58] G. Pratiel, J. Bernadou, B. Meunier. *Adv. Inorg. Chem.*, **45**, 251 (1998).
- [59] A. Dimitrakopoulou, C. Dendrinou–Samara, A.A. Pantazaki, M. Alexiou, E. Nordlander, D.P. Kessissoglou. *J. Inorg. Biochem.*, **102**, 618 (2008).
- [60] D. Li, J. Tian, W. Gu, X. Liu, S. Yan. *J. Inorg. Biochem.*, **104**, 171 (2010).
- [61] J.L. Garcia–Gimenez, M. Gonzalez–Alvarez, M. Liu–Gonzalez, B. Macias, J. Borrás, G. Alzuet. *J. Inorg. Biochem.*, **103**, 923 (2009).
- [62] C. Tolia, A.N. Papadopoulos, C.P. Raptopoulou, V. Psycharis, C. Garino, L. Salassa, G. Psomas. *J. Inorg. Biochem.*, **123**, 53 (2013).

Table 1. Crystallographic data for **1-4**.

	1 [Cd(5-NO ₂ -salo) ₂ (CH ₃ OH) ₂]	2 [Cd(5-NO ₂ -salo) ₂ (phen)]·2CH ₃ OH·H ₂ O	3 [Cd(5-NO ₂ -salo) ₂ (dpamH)]	4 [Cd ₃ (5-NO ₂ -salo) ₆ (bipy) ₂]
Empirical formula	C ₁₆ H ₁₆ Cd ₁ N ₂ O ₁₀	C ₂₈ H ₂₆ Cd ₁ N ₄ O ₁₁	C ₂₄ H ₁₇ Cd ₁ N ₅ O ₈	C ₆₂ H ₄₀ Cd ₃ N ₁₀ O ₂₄
CCDC no.	1055222	1055223	1055224	1055225
Molecular mass	508.71	706.93	615.83	1646.25
Crystal system	Triclinic	Orthorhombic	Triclinic	Triclinic
Temperature (K)	295	295	295	295
Radiation type	Mo K α	Mo K α	Mo K α	Mo K α
Wavelength λ (Å)	0.71073	0.71073	0.71073	0.71073
Space group	P -1	P n n a	P -1	P -1
Unit cell dimensions				
a (Å)	5.1874(2)	7.2025(3)	7.7970(6)	10.5147(16)
b (Å)	7.8388(3)	20.3174(8)	11.3357(9)	11.8775(19)
c (Å)	11.9530(5)	23.2505(8)	13.7461(12)	13.750(2)
α , deg	101.623(2)	90	95.001(3)	100.944(10)
β , deg	94.321(2)	90	98.168(3)	106.419(9)
γ , deg	93.582(2)	90	90.178(3)	107.614(11)
Volume (Å ³)	473.22(2)	3402.39(12)	1197.89(10)	1497.1(2)
Z	1	4	2	1
Absorption coeff. (μ) mm ⁻¹	1.213	0.700	0.972	1.153
Crystal density, Dx, g cm ⁻³	1.78	1.38	1.71	1.83
Crystal size, mm	0.20 × 0.47 × 0.52	0.11 × 0.13 × 0.17	0.22 × 0.25 × 0.33	0.17 × 0.22 × 0.24
θ range for data collection, deg / completeness (%)	2.661-30.687 / 99.8	1.331-32.296 / 87.1	1.502-26.478 / 99.2	1.619-26.682 / 94.5
Range of h, k, l	-7→7, -11→11, -17→17	-9→10, -28→28, -33→33	-9→9, -14→14, 0→17	-13→12, -14→14, -17→17
Measured reflections /	18633 / 2935 / 0.0273	34036 / 5290 / 0.0239	4917 / 3526 / 0.0458	15380 / 5982 / 0.0257

	1 [Cd(5-NO ₂ -salo) ₂ (CH ₃ OH) ₂]	2 [Cd(5-NO ₂ -salo) ₂ (phen)]·2CH ₃ OH·H ₂ O	3 [Cd(5-NO ₂ -salo) ₂ (dpamH)]	4 [Cd ₃ (5-NO ₂ -salo) ₆ (bipy) ₂]
Independent reflections / R _{int}				
No. of parameters	136	197	348	448
Goodness-of-fit on F ² (GOF)	1.000	1.000	1.000	1.000
Final R indices:				
R ₁ , wR ₂ [<i>I</i> > 2σ(<i>I</i>)]	0.0222, 0.0483	0.0541, 0.0923	0.0330, 0.0548	0.0665, 0.1303
R ₁ , wR ₂ (all data)	0.0235, 0.0486	0.1087, 0.1011	0.0571, 0.0620	0.0867, 0.1317
Largest diff. peak / hole (e Å ⁻³)	0.49 / -0.29	0.72 / -0.59	0.50 / -0.45	1.76 / -1.97

Accepted Manuscript

Table 2. Selected bond distances (Å) and angles (°) for **1-4**.

Bond distance (Å)	1	Bond distance (Å)	2	Bond distance (Å)	3	Bond distance (Å)	4
Cd1—O5 ⁱ	2.2828(11)	Cd1—N2 ⁱ	2.325(3)	Cd1—O1	2.254(3)	Cd1—O1	2.220(6)
Cd1—O2 ⁱ	2.2695(12)	Cd1—O2 ⁱ	2.297(2)	Cd1—O2	2.345(3)	Cd1—O2	2.271(6)
Cd1—O1 ⁱ	2.2142(11)	Cd1—O1 ⁱ	2.244(3)	Cd1—O5	2.230(3)	Cd1—O5	2.333(5)
				Cd1—O6	2.319(3)	Cd1—O9	2.305(5)
				Cd1—N3	2.273(3)	Cd1—N4	2.329(7)
Bond angle (°)	1	Bond angle (°)	2	Bond angle (°)	3	Bond angle (°)	4
O5 ⁱ —Cd1—O2 ⁱ	95.47(5)	N2 ⁱ —Cd1—O2 ⁱ	96.55(11)	O1—Cd1—O2	77.47(10)	O1—Cd1—O2	76.1(2)
O5 ⁱ —Cd1—O1 ⁱ	90.46(4)	N2 ⁱ —Cd1—O1 ⁱ	92.65(11)	O1—Cd1—O5	161.15(8)	O1—Cd1—O5	97.9(2)
O2 ⁱ —Cd1—O1 ⁱ	81.26(4)	O2 ⁱ —Cd1—O1 ⁱ	80.73(10)	O2—Cd1—O5	86.77(11)	O2—Cd1—O5	87.6(2)
O5 ⁱ —Cd1—O1	89.54(4)	N2 ⁱ —Cd1—O1	162.00(11)	O1—Cd1—O6	88.02(10)	O1—Cd1—O9	159.6(2)
O2 ⁱ —Cd1—O1	98.74(4)	O2 ⁱ —Cd1—O1	92.67(10)	O2—Cd1—O6	81.27(11)	O2—Cd1—O9	83.8(2)
O1 ⁱ —Cd1—O1	179.995	O1 ⁱ —Cd1—O1	104.09(15)	O5—Cd1—O6	79.33(10)	O5—Cd1—O9	77.4(2)
O5 ⁱ —Cd1—O2	84.53(5)	N2 ⁱ —Cd1—O2	92.12(10)	O1—Cd1—N3	99.42(12)	O1—Cd1—N4	102.9(2)
		O2 ⁱ —Cd1—O2	169.31(14)	O2—Cd1—N3	96.00(12)	O2—Cd1—N4	176.7(2)
		O1 ⁱ —Cd1—O2	92.67(10)	O5—Cd1—N3	92.38(11)	O5—Cd1—N4	89.4(2)
		O1—Cd1—O2	80.73(10)	O6—Cd1—N3	171.38(11)	O9—Cd1—N4	96.9(2)
		N2 ⁱ —Cd1—N2	71.64(15)	O1—Cd1—N4	93.68(10)	O1—Cd1—N5	89.0(2)
		O2 ⁱ —Cd1—N2	92.12(10)	O2—Cd1—N4	170.95(11)	O2—Cd1—N5	110.4(2)
		O1 ⁱ —Cd1—N2	162.00(11)	O5—Cd1—N4	102.28(11)	O5—Cd1—N5	161.83(19)
		O1—Cd1—N2	92.65(11)	O6—Cd1—N4	100.52(11)	O9—Cd1—N5	101.5(2)
						N4—Cd1—N5	72.7(2)
Symmetry :	—	1.5-x, 1-y, z		—		1-y, -z.	

Table 3. UV spectral features of the UV spectra of 5-NO₂-salOH and **1-5** upon addition of DNA (band studied in λ (nm), percentage of hyperchromism or hypochromism $\Delta A/A_0$ (%), blue- or red-shift $\Delta\lambda$ (nm)) and the corresponding DNA binding constants (K_b).

Complex	(λ , nm) ($\Delta A/A_0$ (%) ^a , $\Delta\lambda$ (nm) ^b)	K_b (M ⁻¹)
5-NO ₂ -salOH [32]	366(+> ^c , +5), 430(+>, -5)	5.25(±0.25)×10 ⁵
[Cd(5-NO ₂ -salO) ₂ (CH ₃ OH) ₂], 1	373(-3, -4), 432(-21, -10)	3.45(±0.40)×10 ⁵
[Cd(5-NO ₂ -salO) ₂ (phen)], 2	373(-1, -4), 432(-12.5, -7)	2.54(±0.42)×10 ⁵
[Cd(5-NO ₂ -salO) ₂ (dpamH)], 3	370(-3.5, -4), 430(-16.5, -6)	1.65(±0.10)×10 ⁶
[Cd ₃ (5-NO ₂ -salO) ₆ (bipy) ₂], 4	373(-3.5, -4), 431(-14, -7)	5.29(±0.15)×10 ⁴
[Cd(5-NO ₂ -salO)(neoc)(NO ₃) ₂], 5	373(-0.5, -4), 431(-14.5, -7)	3.25(±0.20)×10 ⁴

^a “+” denotes hyperchromism and “-” denotes hypochromism

^b “+” denotes bathochromism and “-” denotes hypochromism

^c “+>” denotes extreme hyperchromism

Accepted Manuscript

Table 4. Percentage of EB–DNA fluorescence emission quenching ($\Delta I/I_0$, %) and Stern–Volmer constants (K_{SV} , in M^{-1}) for 5–NO₂–saloH and **1-5**.

Compound	$\Delta I/I_0$ (%)	K_{SV} (M^{-1})
5–NO ₂ –saloH	72.5	$2.22(\pm 0.06) \times 10^5$
[Cd(5–NO ₂ –salo) ₂ (CH ₃ OH) ₂], 1	86.7	$1.41(\pm 0.03) \times 10^6$
[Cd(5–NO ₂ –salo) ₂ (phen)], 2	80.4	$7.37(\pm 0.25) \times 10^5$
[Cd(5–NO ₂ –salo) ₂ (dpamH)], 3	67.1	$1.21(\pm 0.05) \times 10^5$
[Cd ₃ (5–NO ₂ –salo) ₆ (bipy) ₂], 4	69.5	$5.90(\pm 0.25) \times 10^5$
[Cd(5–NO ₂ –salo)(neoc)(NO ₃) ₂], 5	62.4	$5.86(\pm 0.24) \times 10^5$

Accepted Manuscript

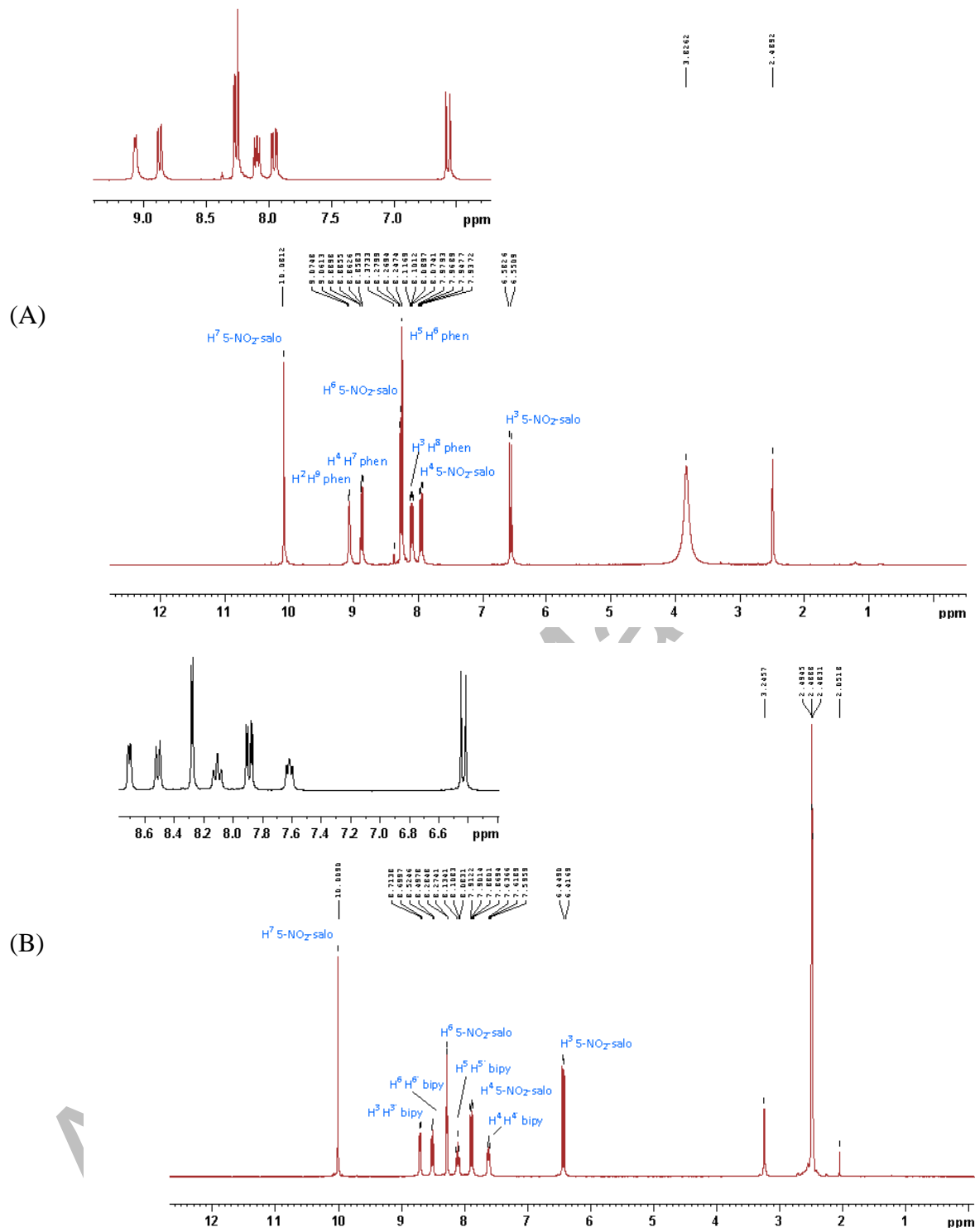


Figure 1. ¹H-NMR spectra of (A) **2** and (B) **4** in DMSO-d₆.

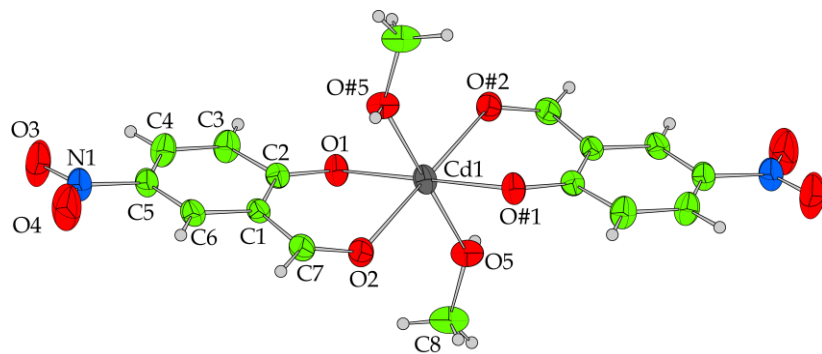


Figure 2. Molecular structure of $[\text{Cd}(5\text{-NO}_2\text{-salo})_2(\text{CH}_3\text{OH})_2]$ (**1**) with the displacement ellipsoids shown at the 50% probability level.

Accepted Manuscript

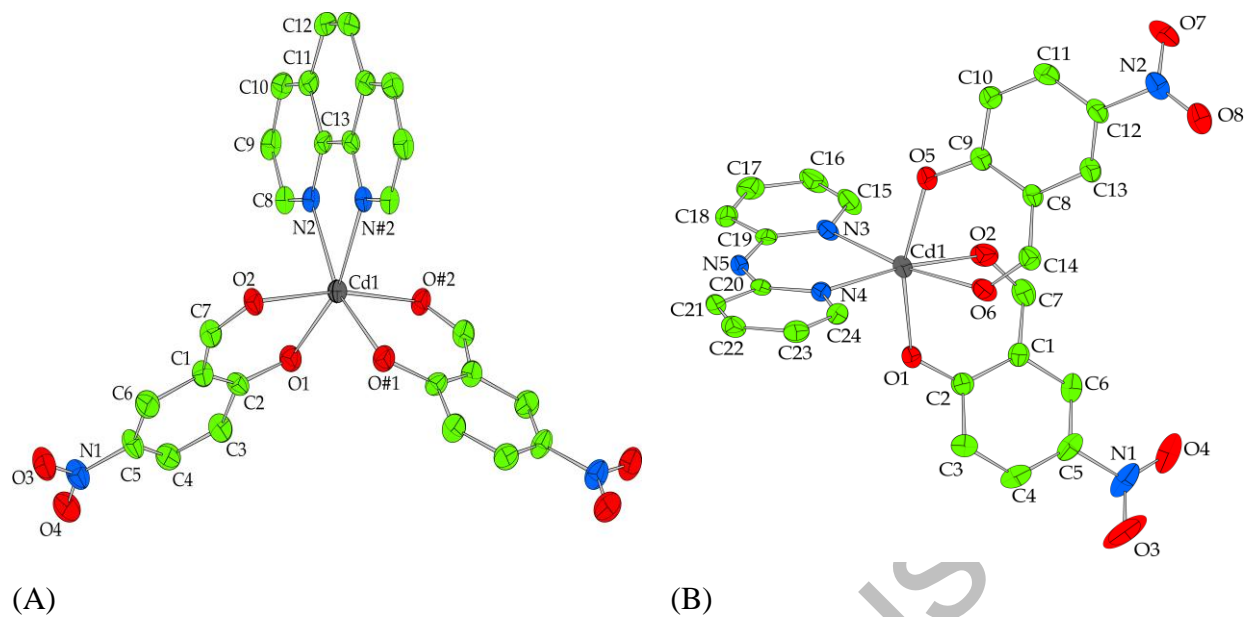


Figure 3. Molecular structure of (A) $[\text{Cd}(5\text{-NO}_2\text{-salo})_2(\text{phen})]\cdot 2\text{CH}_3\text{OH}\cdot\text{H}_2\text{O}$ (**2**) and (B) $[\text{Cd}(5\text{-NO}_2\text{-salo})_2(\text{dpamH})]$ (**3**), with the displacement ellipsoids shown at the 50% probability level. The hydrogens are omitted for clarity.

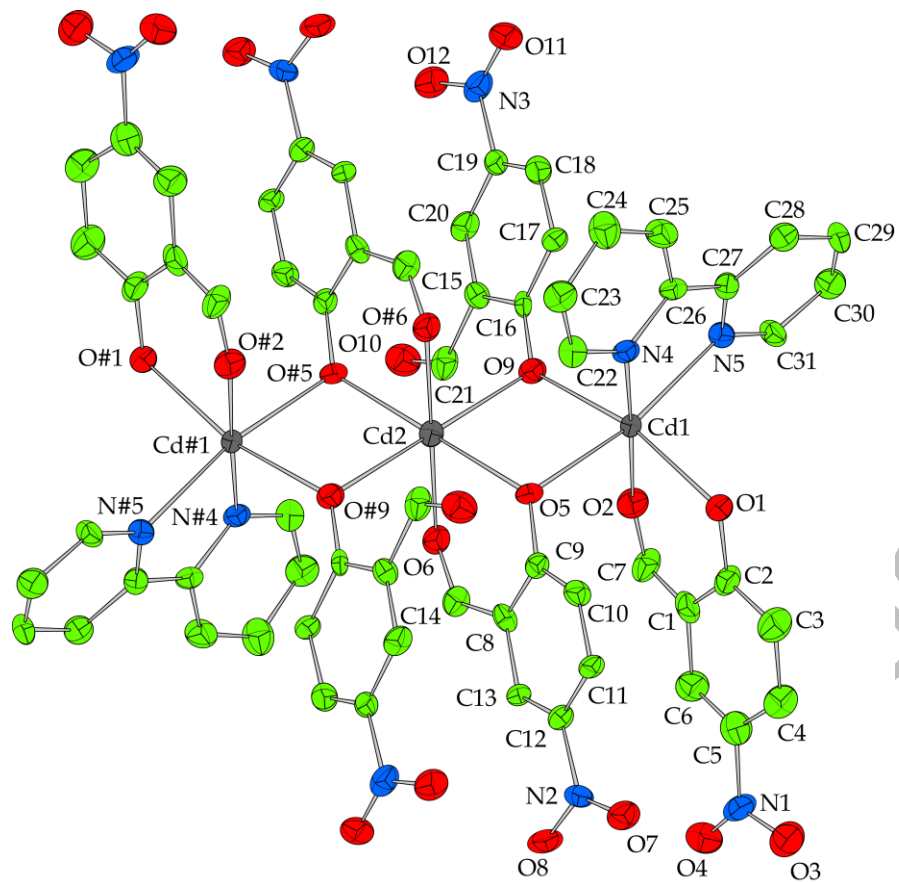
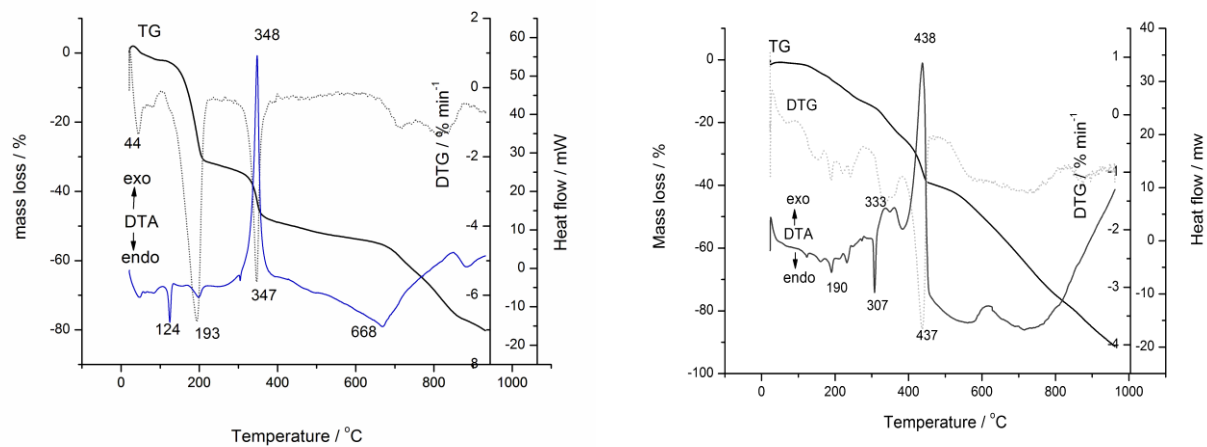


Figure 4. Molecular structure of $[Cd_3(5\text{-NO}_2\text{-salo})_6(\text{bipy})_2]$ (**4**) with the displacement ellipsoids shown at the 50% probability level. The hydrogens are omitted for clarity.



(A)

(B)

Figure 5. Thermoanalytical curves (TG/DTG-DTA) of (A) $[\text{Cd}(5\text{-NO}_2\text{-salo})_2(\text{MeOH})_2]$ (**1**) and (B) $[\text{Cd}(5\text{-NO}_2\text{-salo})_2(\text{phen})]\cdot 2\text{CH}_3\text{OH}\cdot\text{H}_2\text{O}$ (**2**).

Accepted Manuscript

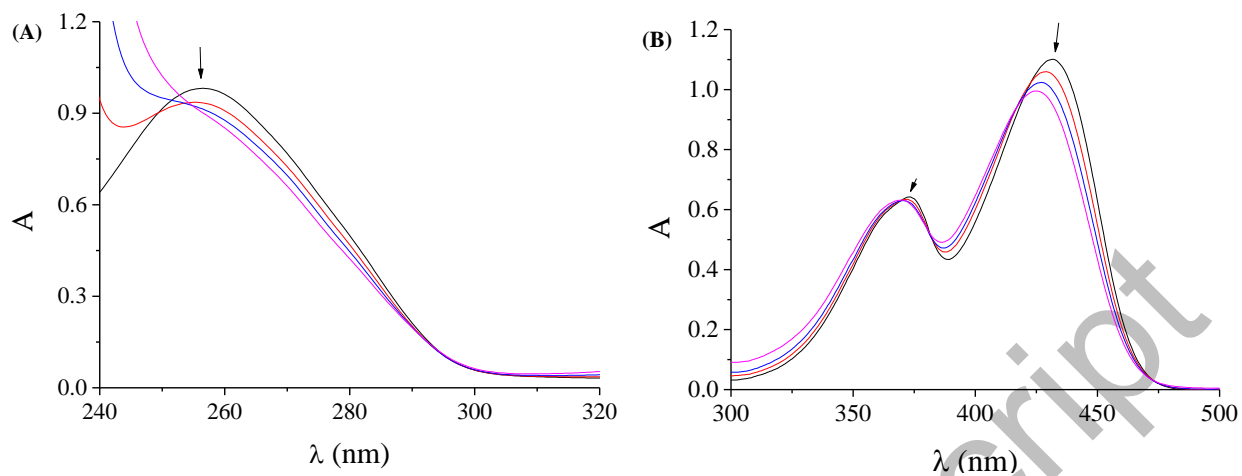


Figure 6. (A) UV spectra of CT DNA (1.48×10^{-4} M) in buffer solution (150 mM NaCl and 15 mM trisodium citrate at pH 7.0) in the absence or presence of **2** at increasing amounts. The arrow shows the changes upon increasing amounts of the complex. (B) UV spectra of DMSO solution (2×10^{-5} M) of **1** in the presence of increasing amounts of CT DNA. The arrows show the changes upon increasing amounts of CT DNA.

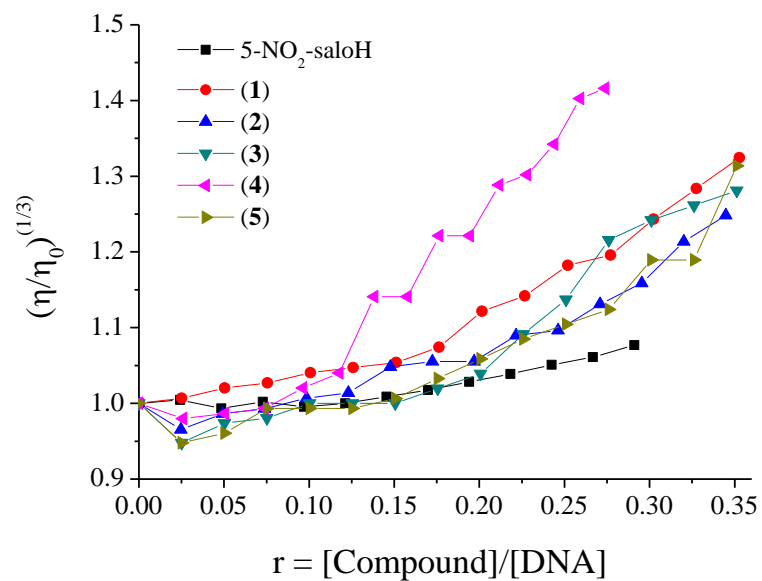


Figure 7. Relative viscosity $(\eta/\eta_0)^{1/3}$ of CT DNA (0.1 mM) in buffer solution (150 mM NaCl and 15 mM trisodium citrate at pH 7.0) in the presence of 5-NO₂-salOH and **1-5** with increasing amounts (up to $r = [\text{compound}]/[\text{DNA}] = 0-0.35$).

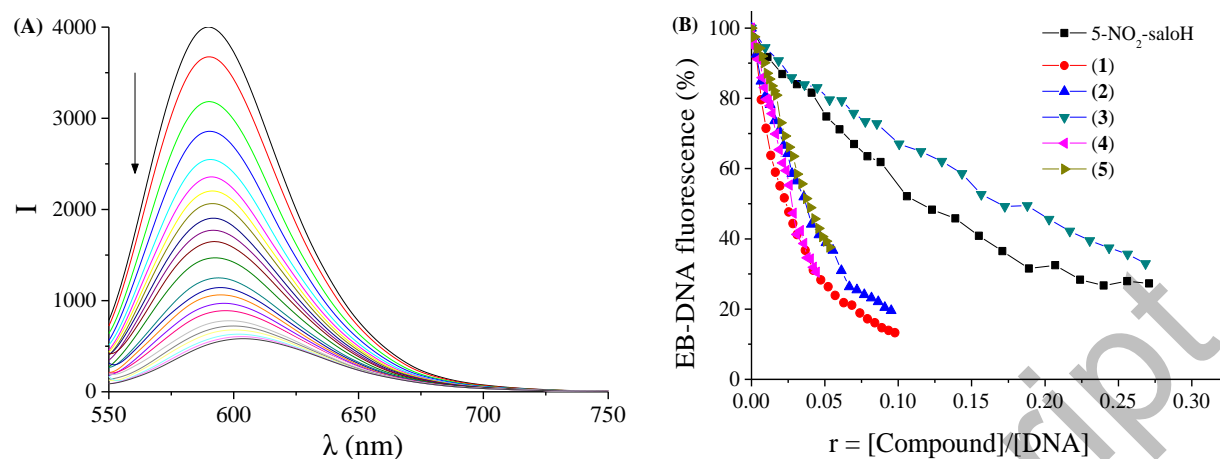


Figure 8. (A) Fluorescence emission spectra ($\lambda_{\text{excitation}} = 540 \text{ nm}$) for EB–DNA ($[\text{EB}] = 20 \mu\text{M}$, $[\text{DNA}] = 26 \mu\text{M}$) in buffer solution in the absence and presence of increasing amounts of **1** (up to $r = 0.1$). The arrow shows the changes of intensity upon increasing amounts of **1**. (B) Plot of EB relative fluorescence emission intensity at $\lambda_{\text{emission}} = 592 \text{ nm}$ (%) vs r ($r = [\text{complex}]/[\text{DNA}]$) (150 mM NaCl and 15 mM trisodium citrate at pH = 7.0) in the presence of 5-NO₂-saloH and **1-5** (up to 13.3% of the initial EB–DNA fluorescence intensity for **1**, 19.6% for **2**, 32.9% for **3**, 30.5% for **4** and 37.6% for **5**).

Graphical Abstract

